Int. J. Electrochem. Sci., 13 **(2018)** 7517 – 7531, doi: 10.20964/2018.08.60

International Journal of
ELECTROCHEMICAL
SCIENCE
www.electrochemsci.org

β-amino Acid-Derived Triazols as Corrosion Inhibitors for API 5L X52 Steel Immersed in 1 M HCl

A. Espinoza-Vazquez[1], *F. J. Rodríguez Gómez*[1], *E. Juaristi*[4,5], *M. Escudero-Casao*[4], *Guillermo E. Negrón-Silva*[2,*], *D. Ángeles-Beltrán*[2], *M. Palomar-Pardavé*[3]

[1] Facultad de Química, Universidad Nacional Autónoma de México, Av. Universidad No. 3000, Coyoacán, C.U., México, Ciudad de México, CP 04510, México.
[2] Universidad Autónoma Metropolitana Azcapotzalco. Departamento de Ciencias Básicas, México, Ciudad de México., C.P. 02200.
[3] Universidad Autónoma Metropolitana-Azcapotzalco, Departamento de Materiales, Av. San Pablo 180 Col. Reynosa-Tamaulipas, C.P. 02200 Ciudad de México.
[4] Departmento de Química, Centro de Investigación y de Estudios Avanzados, Avenida IPN # 2508, 07360 México City, México.
[5] El Colegio Nacional, Luis González Obregón 23, Centro Histórico, 06020 México City, México
[*]E-mail: gns@correo.azc.uam.mx

Received: 5 April 2018 / *Accepted:* 6 June 2018 / *Published:* 5 July 2018

The corrosion inhibition of API 5L X52 steel immersed in a 1 M HCl aqueous solution, due to three β-amino acid-derived triazols in stagnant conditions at 298 K, was evaluated using electrochemical impedance spectroscopy and polarization resistant techniques. The effect of triazol concentration and immersion time was evaluated. For all cases, it was found that the inhibition efficiency (η) increased with the triazol concentration. Compounds **1** and **2** exhibited η values ranging from 80% to 97%. An adsorption-type analysis was also performed on the metallic surface using the Langmuir isotherm, demonstrating that the process is combined for organic compounds **1** and **3**, whereas the process exhibits chemisorption when inhibitor **2** is evaluated. For long immersion times, the organic inhibitor (compound 1) showed good corrosion protection for 224 hours of immersion, with η > 90%. Finally, it was demonstrated by SEM that the corrosion velocity is diminished using the compound **1** inhibitor at 50 ppm.

Keywords: β-amino acids, triazols, EIS, API 5L X52

1. INTRODUCTION

The oil industry uses various metallic materials to extract, transport, process and store products of interest from oil wells to shipping terminals, including the stages of processing and storage [1,2]. Generally, structures made from these metallic materials are affected by both external and internal

corrosion phenomena. CO_2 and H_2S are the most important corrosive species [3] and are in equilibrium with three phases: oil, water and gas; thus, the amounts of CO_2 and H_2S in each phase are related, with different concentrations given by the solubilities corresponding to each phase. In this regard, HCl is used for stimulation in oil wells to prevent clogging [4]. It is important to note that this acid is capable of dissolving the passive film on the surface of the metal, leaving it in an active state, facilitating the corrosion process. Alternatively, oxygen plays an important role in corrosion, meaning that it is almost impossible to prevent it. It is increasingly evident that controlling corrosion is the most economical solution.

One of the most relevant technologies for corrosion control consists of the use of organic corrosion inhibitors [5-7]; as a consequence, a great deal of research has been done to generate compounds that can function as efficient inhibitors and can be environment friendly [8]. In the present literature, these compounds are said to present the capacity to be adsorbed on a metallic surface, which is related to the existence of nitrogen and oxygen heteroatoms, as well as to the π electronic density in their structures [9-10]. Thus, it is important to determine the performance of these compounds to guarantee their effectiveness and to ensure system integrity by allowing sufficient immersion times to determine if the inhibitors are permissible for use during normal operations.

Previously, we demonstrated that several triazols derived from nucleobases are rather efficient corrosion inhibitors [11]. In the specialized bibliography, there are a few studies on corrosion inhibition of triazols derived from α-amino acids [12], but there are none on triazols derived from β-amino acids [13]. Recently, some amino acid-derived 1,2,3 triazols, with potential applications as optical probes to detect proteins, have been described [14]. The main objective of this work is to study the effect of the concentration of compounds **1-3** for use as corrosion inhibitors under static conditions and to determine the effect of immersion time in an acid medium.

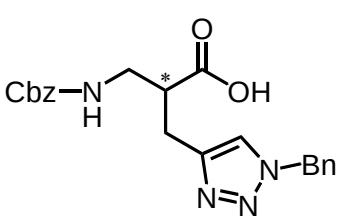

racemic mixture

1

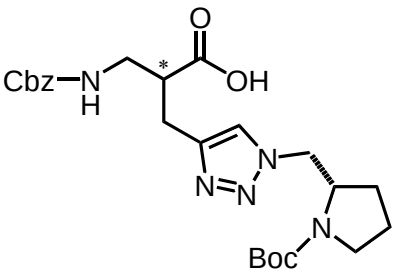

(*S*,*S*) and (*R*,*S*) diastereomeric mixture 1:1

2

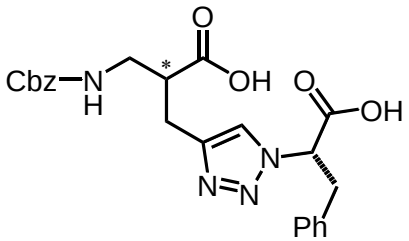

(*S*,*S*) and (*R*,*S*) diastereomeric mixture 1:1

3

Figure 1. Chemical structures of the triazol-containing β-amino acids 1-3.

2. EXPERIMENTAL METHODOLOGY

2.1 Synthesis and characterization of the triazole-containing β-amino acids

The three mixtures of β-amino acids employed in the present study (Figure 1) are: *rac*-3-(1-benzyl-1H-1,2,3-triazol-5-yl)-2-(((benzyloxycarbonyl)amino)methyl)propanoic acid (compound **1)**, diastereomeric mixture 1:1 of (*S*)-3-(((benzyloxy)carbonyl)amino)-2-((1-(((*S*)-1-(*tert*-butoxycarbonyl)pyrrolidin-2-yl)methyl)-1H-1,2,3-triazol-4-yl)methyl)propanoic acid and (*R*)-3-(((benzyloxy)carbonyl)amino)-2-((1-(((*S*)-1-(*tert*-butoxycarbonyl) pyrrolidin-2-yl)methyl)-1H-1,2,3-triazol-4-yl)methyl)propanoic acid (compound **2**), and diastereomeric mixture 1:1 of (*S*)-3-(((benzyloxy)carbonyl)amino)-2-((1-((*S*)-1-carboxy-2-phenylethyl)-1H-1,2,3-triazol-4-yl)methyl)propanoic acid and (*S*)-3-(((benzyloxy)carbonyl)amino)-2-((1-((*R*)-1-carboxy-2-phenylethyl)-1H-1,2,3-triazol-4-yl)methyl)propanoic acid (compound **3**). These were synthesized and duly characterized.

The synthesis of these molecules via the Click Cycloaddition Reaction was recently reported and includes the proper characterization of compounds **1** and **2**, including information from IR, NMR and high-resolution mass spectra (HRMS) techniques. The mixture of compound **3** was prepared from the standard deprotection of the corresponding methyl esters (Scheme 1) [13].

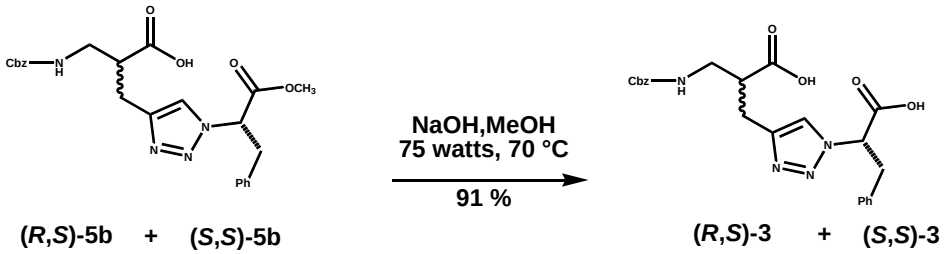

Scheme 1. Synthesis of the diastereomeric mixture 3 from basic hydrolysis of the previous characterized methyl ester **5b** under microwave conditions [13].

The diastereomeric mixture 1:1 of (*S*)-3-(((benzyloxy)carbonyl)amino)-2-((1-((*S*)-1-carboxy-2-phenylethyl)-1H-1,2,3-triazol-4-yl)methyl)propanoic acid and (*S*)-3-(((benzyloxy)carbonyl)amino)-2-((1-((*R*)-1-carboxy-2-phenylethyl)-1H-1,2,3-triazol-4-yl)methyl)propanoic acid, diastereomeric mixture **3**. To a stirred solution of (*S*)-3-(((Benzyloxy)carbonyl)amino)-2-((1-((*S*)-1- methoxy-1-oxo-3-phenylpropan-2-yl)-1H-1,2,3-triazol-4- yl)methyl)propanoic acid and (*R*)-3-(((Benzyloxy) carbonyl)amino)-2-((1-((*S*)-1-methoxy-1-oxo-3-phenylpropan-2-yl)-1H-1,2,3-triazol-4-yl)methyl)propanoic acid **5b** [13] (0.6 g, 1.28 mmol, 1 equiv.) in methanol (50 mL) was added NaOH (0.128 g, 3.21 mmol, 2.5 equiv.) in a minimal amount of water. The resulting solution was heated to reflux under microwave irradiation (75 watts, 70 °C) for 60 min. The solvent was removed at reduced pressure, and the residue was diluted with water (50 mL) and EtOAc (50 mL). The aqueous layer was slowly acidified to pH 2 with 6 M HCl, and the product was extracted with ethyl acetate (2 x 50 mL). The combined organic layer was washed with brine (50 mL) and dried over anhydrous Na_2SO_4, and

the solvent was evaporated at reduced pressure. The crude compound was purified by column chromatography (CH_2Cl_2/Methanol/AcOH, 95:5:0.1) to yield a mixture of diastereoisomers **3** as a yellow oil (0.526 g, 91%).

^{1}H NMR (500 MHz, $CDCl_3$) δ 10.92 (br, 4H), 7.53 (s, 1H),7.47(s, 1H), 7.32-7.25 (m, 10H), 7.15-7.14 (m, 6H), 6.96 (m, 4H), 5.73 (br, NH, 2H), 5.52 (m, 2H), 5.16(m, 2H), 5.05 (s, 2H), 3.38-3.29 (m, 8H), 2.96-2.91 (m, 6H). **^{13}C NMR (125 MHz, $CDCl_3$)**: δ 177.9,177.8, 171.4, 171.3, 158.2, 157.1, 143.8, 143.7, 136.3, 135.8, 135.0, 134.8, 128.9, 128.8, 128.7, 128.6, 128.1, 127.5, 123.5, 123.4, 67.9, 67.1, 64.5, 64.4, 45.6, 45.5, 41.2, 41.0, 38.5, 38.9, 24.6, 24.5. **HR-ESI-TOF** Calcd. for $C_{23}H_{25}N_4O_6$ ($M+H^+$), 453.1774, found: 453.1795.

2.2 Electrochemical measurements

A solution of 0.01 M of compounds **1**, **2** and **3** (Figure 1) was prepared in ethanol, and subsequently, aliquots (10-100 ppm) of each inhibitor compound were added to 50 mL of 1 M HCl.

Electrochemical impedance spectroscopy (EIS) was conducted with Zennium-Zanher equipment applying a sinusoidal potential of ±10 mV in a frequency interval (100 KHz at 0.01 Hz) in a three-electrode electrochemical cell with 0 ppm to 100 ppm of the inhibitor in a corrosive solution of 1 M HCl. The working electrode was API 5L X52 steel (Area= 0.196 cm^2), the reference electrode was a saturated Ag /AgCl electrode, and the counter electrode was a graphite rod. The tests were performed in triplicate, and before running the EIS test, the potential was stabilized for 1500 seconds. Afterwards, for the polarization curve test, a sweep of 60 mV/s over a range from -500 mV to 500 mV was performed using a Gill ACM potentiostat and the ACM analysis software for data interpretation. After identifying the best inhibitor (compound **1**) at the 50 ppm level, measurements were performed using EIS for different immersion times from 24 hours to a maximum period of 504 hours.

2.3. Surface characterization

The API 5L X52 steel surface was prepared both without (blank) and with an inhibitor (compound 1). A 50ppm concentration was used for a 24-h immersion time. After the experiment, the steel was washed with distilled water and dried, and then the surface was analyzed using scanning electron microscopy (SEM) with a Carl-Zeiss microscope SUPRA 55 VP at 10 kV with a 300X secondary electron detector.

3. RESULTS DISCUSSION

3.1. EIS measurements

Figure 2 shows the Nyquist diagram of the steel without any inhibitor, which reached a Z_{re} value of ~ 30 Ω cm^2.

Figure 3 shows the Nyquist diagrams corresponding to the β-amino acids already shown in figure 1 for static conditions.

The Nyquist diagram for figure 3a (inhibitor **1)** is the best, as it has the longest diameter of semicircles (Z_{real}) from low concentrations, which is attributed to the presence of the benzyl group in the N1 of the triazole ring, which can foster the adsorption process of the inhibitor over the metallic surface. According to the form in which these semicircles are presented, there is a time constant relating the resistance to the charge transference for compounds **1** and **3** (Figures 3a and 3c) [15]. In contrast, the semicircles formed are not perfect, and their behavior is characteristic of solid electrodes, which is attributed to the homogeneity and roughness of the surface [16].

Compound **2** (figure 3b) exhibits the highest R_{ct} value of 604.5 **Ω**cm^2 at 100 ppm. It is possible to observe that the form of the semicircle is depressed, which may be attributed to the presence of two-time constants, one related to the charge transference resistance and the other to the adsorbed organic molecules [17].

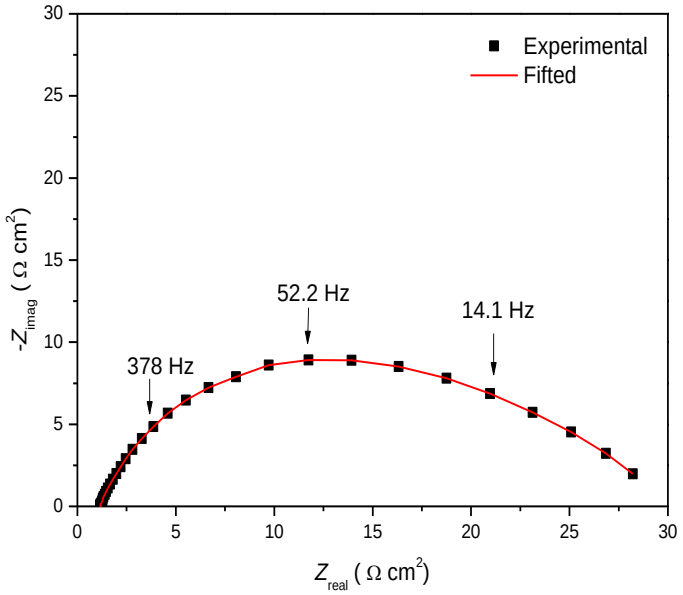

Figure 2. Nyquist diagram for API 5L X52 steel immersed in 1 M HCl without any inhibitor.

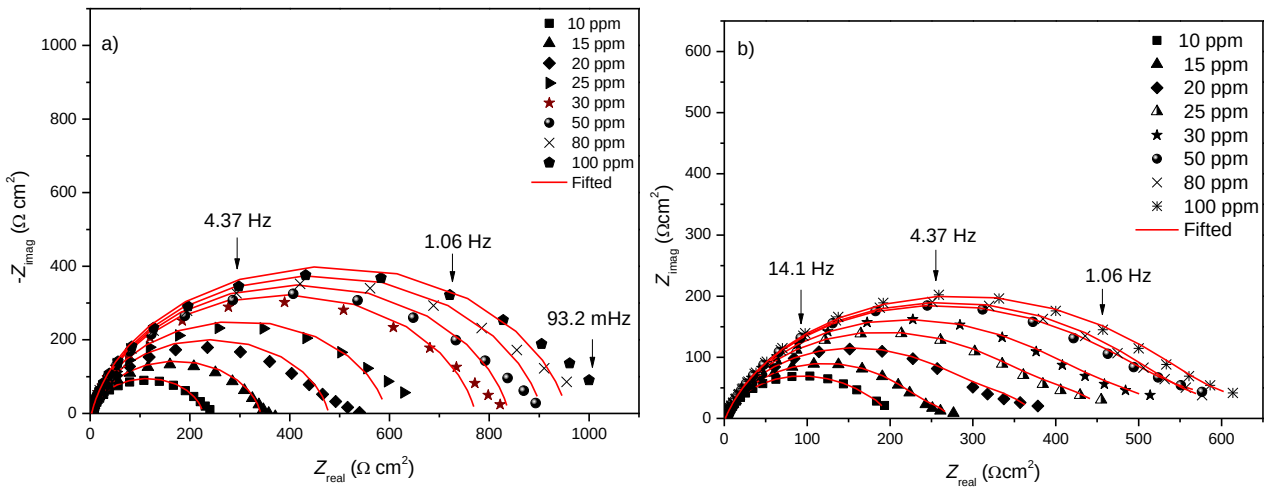

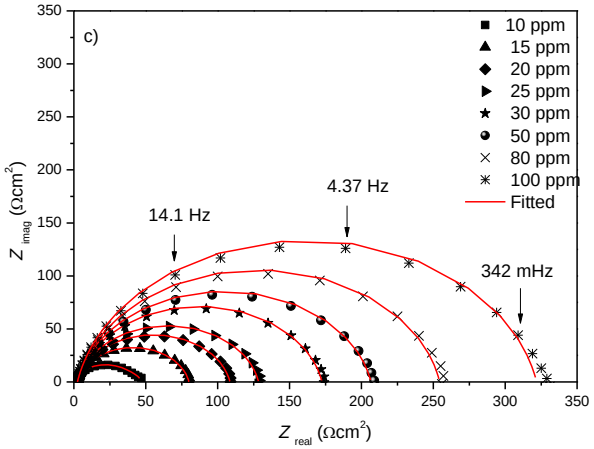

Figure 3. Nyquist diagram of the β-amino acids derived triazols: a) compound **1**, b) compound **2**, and c) compound **3** on API 5L X52 steel in 1 M HCl.

Using the equivalent electric circuit shown in figures 4a and 4b, the electrochemical parameters were determined (as own in Table 1) for the different studied concentrations of compounds 1 to 3.

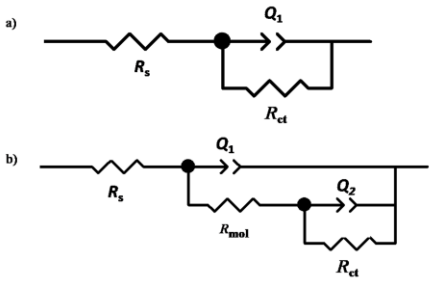

Figure 4. Equivalent electric circuit used in the system with and without the inhibitor.

Here, R_s is the resistance from the solution, R_{ct} is the resistance from charge transference and Q is the constant phase element, R_{mol} is the resistance from the adsorbed organic molecules.

Generally, the double layer behaves as a constant phase element (CPE) instead of a pure capacitor. The CPE parameter is adjusted to more precisely fit the semicircle (equation 1a). To calculate the capacitance values, equation (1b) was used [18-20]:

$$Z_{CPE}=Q^{-1}(j\omega)^{-n}, \quad (1a)$$

where C_{dl} represents a double layer capacitance (equation 2b),

$$C_{dl} = Y0\ (\omega''_m)^{n-1}, \quad (1b)$$

where Q represents the value of the CPE, n is the exponent of the CPE (which can be used as an indicator of the heterogeneity or roughness in the surface) and ω''_m is the angular frequency in rad/s. Depending on n, the CPE can represent a resistance (Z_{CPE} = R, n = 0), a capacitance (Z_{CPE} = C, n = 1), a Warburg impedance (Z_{CPE} = W, n = 0.5) or an inductance (Z_{CPE} = L, n = -1). The inhibition efficiency (η) [21-23] is given by equation 2:

$$\eta(\%) = \frac{\left(\frac{1}{Rp}\right)\text{blank} - \left(\frac{1}{Rp}\right)\text{inhibitor}}{\left(\frac{1}{Rp}\right)\text{blank}} x\ 100 \quad (2)$$

R_p Blank = Polarization resistance without an inhibitor,
R_p Inhibitor = Polarization resistance in the presence of an inhibitor.

The values of the polarization to resistance are determined as:

$$R_p = R_{mol} + R_{ct.} \quad (3)$$

In Table 1, variations in the inhibition efficiency are evaluated under static conditions for the β-amino acids. Compound **1**, with a concentration of 15 ppm, reached 91% of η, whereas the same concentrations for compounds **2** and **3** reached values of η of approximately 98% and 63%, respectively.

The R_p values increased with the inhibitor concentration, and we noted that the electrode surface exhibited a greater protection against corrosion [24].

The addition of the inhibitor to the corrosive solution decreased the double layer electrochemical capacitance (C_{dl}). The double layer between the charged metal surface and the solution is considered a condenser. The adsorption over the API 5L X52 steel surface decreases the electric capacity of moving water molecules and other ions adsorbed on the surface. This decrease is related to the capacity of the metallic surface being inhibited by the organic compound, which forms a protective film [25-27].

Table 1. Electrochemical parameters for the corrosion inhibitor compounds on API 5L X52 steel for static conditions immersed in 1 M HCl

Compound	C (ppm)	R_s (Ωcm^2)	±SD	n	C_{dl} (μFcm^{-2})	±SD	R_p (Ωcm^2)	±SD	η (%)	±SD
1	10	2.8	0.2	0.9	87.3	5.4	269.1	16.7	88.8	0.7
	15	2.7	0.0	0.9	90.4	0.7	332.9	4.3	91.0	0.1
	20	3.0	0.3	0.8	85.4	7.8	522.8	47.5	94.2	0.5
	25	3.0	0.3	0.9	80.2	7.3	677.1	62.7	95.5	0.4
	30	3.0	0.3	0.9	78.4	8.0	844.4	74.6	96.4	0.3
	50	3.0	0.3	0.9	73.7	4.5	918.2	81.2	96.7	0.3
	80	3.0	0.3	0.9	74.7	8.4	991.3	86.7	97.0	0.3
	100	3.1	0.3	0.9	71.8	6.5	1049.6	95.5	97.1	0.3
2	10	5.8	0.3	0.9	21.7	1.0	182.9	18.3	83.6	0.1
	15	5.9	0.3	0.9	19.5	1.2	258.3	18.5	88.4	0.1
	20	5.8	0.3	0.8	21.1	1.1	341.8	22.0	91.2	0.0
	25	5.8	0.3	0.9	20.2	2.3	412.0	13.0	92.7	0.0
	30	5.9	0.3	0.9	20.3	1.4	475.3	26.0	93.7	0.0
	50	6.1	0.3	0.9	19.7	0.9	557.1	67.8	94.6	0.1
	80	6.3	0.3	0.9	19.3	1.0	569.4	68.5	94.7	0.0
	100	6.5	0.3	0.9	19.2	0.9	604.5	73.5	95.0	0.0
	10	2.2	0.1	0.9	106.7	6.9	43.3	1.5	30.6	2.4
	15	2.5	0.2	0.9	98.0	6.1	81.7	3.6	63.2	1.6

	20	2.5	0.2	0.8	79.6	5.8	111.8	5.1	73.1	1.2
3	25	2.5	0.1	0.9	84.4	3.9	133.1	6.4	77.4	1.1
	30	2.5	0.2	0.9	87.4	6.0	179.1	8.1	83.2	0.8
	50	2.5	0.2	0.9	85.7	5.9	214.9	9.7	86.0	0.6
	80	2.5	0.1	0.9	90.4	4.3	265.8	12.7	88.7	0.5
	100	2.5	0.2	0.9	101.9	6.6	336.2	15.2	91.1	0.4

±SD Standard Deviation

In figure 5, the values of the inhibition efficiency at different concentrations of the three β-amino acids under study are shown. The best corrosion inhibitor is compound **1**, which has an η that is greater than 95% for a concentration of 25 ppm, which fulfils the PEMEX norm NRF-005-PEMEX-2009.

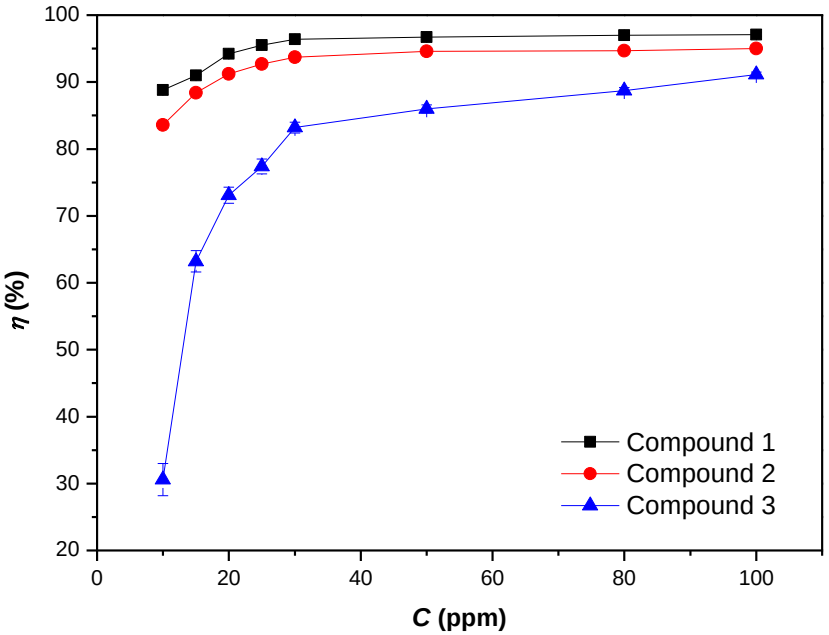

Figure 5. Variations in the inhibition efficiency with the concentration of the β-amino acid triazols (compounds **1-3**, Figure 1) immersed in 1 M HCl.

3.2. Effect of immersion time

After observing that the best inhibitor is compound **1** by means of EIS, different measurements with long immersion times (504 hours) were performed to observe the behavior of the formed film.

In Table 2, it is possible to observe that the R_p value increased after 72 hours of immersion, which is attributed to the fact that this is the time needed for the inhibitor molecules to completely adsorb [28-29]. After this time, an inhibitor desorption process starts, and the R_p value begins to decrease slightly. Despite this, at 336 hours, the process still presents good effectiveness against corrosion.

Table 2. Electrochemical parameters for compound **1** as a corrosion inhibitor on API 5L X52 steel as a function of immersion time

t (h)	R_s (Ωcm^2)	n	C_{dl} (μFcm^{-2})	R_p (Ωcm^2)	η (%)
1	1.2	0.9	19.7	1421.3	98.9
24	1.2	0.9	19.5	1732.0	98.3
72	1.6	0.9	21.4	1221.0	97.5
120	1.2	1.0	49.4	770.7	96.1
168	1.6	1.0	10.9	945.0	96.8
240	1.3	1.0	11.2	495.0	93.9
336	2.5	0.9	28.4	210.2	85.7
504	3.3	0.8	93.1	47.0	36.2

3.3. Polarization measurements

In figure 6, the potentiodynamic polarization curves are depicted both in the absence of an inhibitor and with a concentration of 100 ppm. The corrosion potential (E_{corr}), corrosion current density (i_{corr}), Tafel anodic slopes (b_a), Tafel cathodic slopes (b_c), and inhibition efficiency (η) are presented in Table 3.

The inhibition efficiency of the organic compounds (triazols) **1**-**3** were calculated by:

$$\eta = (1 - \frac{i\,corr_{inhibitor}}{icorr_{uninhibitor}}) \text{ x } 100, \qquad (4)$$

where $i$corr$_{inhibitor}$ is the corrosion current density with an inhibitor and $i$corr$_{uninhibited}$ is the corrosion current density in the absence of an inhibitor.

It is possible to observe that the corrosion speeds (i_{corr}) decrease in the presence of the inhibitor. Comparing the results from electrochemical impedance spectroscopy, similar efficiencies are determined, which corroborate the values obtained. The corrosion potential becomes more negative after adding the corrosion inhibitor, and the largest difference is 277 mV between the solution with and without 100 ppm of compound **3**, meaning that the reaction to corrosion was inhibited [30].

In recent articles, it has been reported that if the corrosion potential (E_{corr}) does not exceed ±85 mV, the inhibitor is classified as a mixed type. Compounds **1** and 3 are classified as cathodic types, whereas for inhibitor **2**, the difference in E_{corr} does not exceed this limit, meaning it is classified as a mixed type [31].

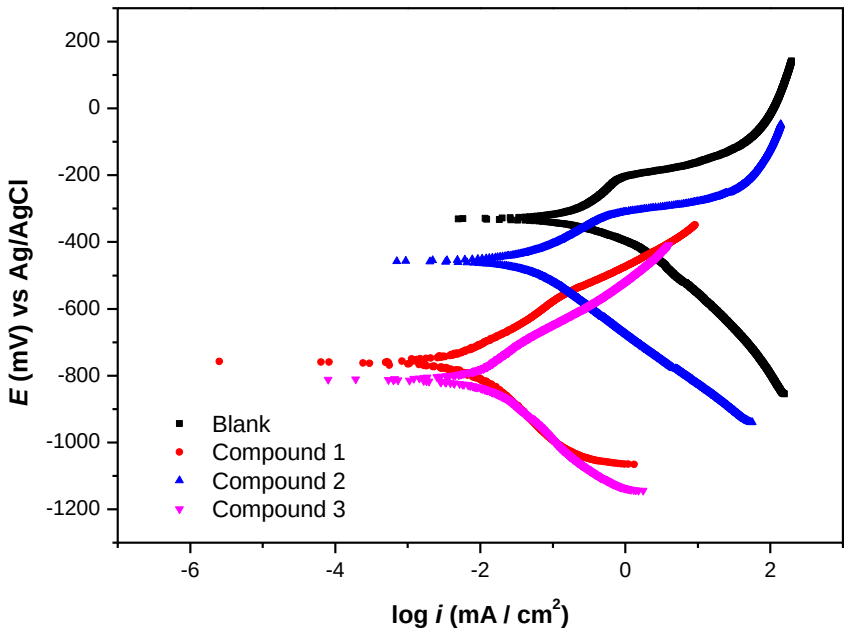

Figure 6. Polarization curves with and without an inhibitor for API 5L X52 steel immersed in 1 M HCl

Table 3. Electrochemical parameters obtained from the polarization resistance curves for API 5 X52 steel immersed in 1 M HCl

Inhibitor	*C* (ppm)	E_{corr} (mV) vs Ag/AgCl	b_c (mV dec^{-1})	b_a (mV dec^{-1})	i_{corr} (mA/cm^2)	θ	η (%)
Blank	0	-465.3	173.4	125.1	0.53	-	-
1	100	-758.1	184.5	146.2	0.01	0.52	98.9
2	100	-452.9	159.6	119.8	0.04	0.45	92.2
3	100	-808.5	125.7	146.1	0.01	0.52	98.7

In Table 4, some organic compounds used as corrosion inhibitors are shown. These compounds are obtained by organic synthesis [32-36] and leave extracts [37-41]. It is necessary to highlight that most of these compounds require very high concentrations (> 50 ppm) to inhibit corrosion, and in some cases, their effectiveness is not good when evaluated under static conditions.

Comparing these data with compounds 1 and 2 shows good protection against corrosion in the 1 M HCl medium, with η > 89% from 10 ppm. However, other important parameters that the literature have not taken into account are different immersion time conditions (film persistence). Compound 1 was effective for 336 hours at 50 ppm (η close to 85%).

Table 4. Inhibition efficiencies of organic compounds used as corrosion inhibitors in carbon steel immersed in 1 M HCl.

Inhibitor	**Steel**	**Concentration (ppm)**	***η* (%)**
3-Amino alkylated indoles[32]	Mild steel	96	84.7
pyrazolone derivatives [33]	N80 steel	150	85.4
6-(4-hydroxyphenyl)-3-mercapto-7,8-dihydro-[1,2,4] triazolo[4,3-b][1,2,4,5]tetrazine[34]	Mild steel	1250	74.0
nonionic surfactants[35]	X65 steel	565	78.3
Hidrazine derivatives[36]	Mild steel	220	62.4
Musa paradisica peel extract [37]	Mild steel	100	81.0
Artemisia Mesatlantica essential oil [38]	C35E Carbon steel	1200	78.9 (after 6 hours of immersion)
Nigella sativa [39]	Iron	250	81.9
Watermelon waste [40]	Mild steel	2000	86.0
Ginkgo leaf extract [41]	X70 steel	200	90.0

3.4. Adsorption Isotherms

To explain the types of adsorption occurring in the β-amino acids being studied here, several different descriptive models are used [42-44]. One of the most important is:

a) Langmuir isotherm, which uses monolayer (monomolecular) adsorption and is determined from equation 5:

$$\frac{C}{\theta} = \frac{1}{k_{ads}} + C \,, \qquad (5)$$

where Θ is the degree of coating, C is the inhibitor concentration, and k_{ads} is the equilibrium constant obtained from a linear adjustment.

The values for the degree of coating (Θ) can be obtained from equation 6:

$$\theta = \frac{\eta}{100}. \qquad (6)$$

After analyzing which isotherm best describes the behavior of the inhibitors used, the Gibb´s standard energy of adsorption is calculated [45-46]:

$$\Delta G°\text{ads} = -55.5\, RT \ln \text{k ads}, \qquad (7)$$

where R is the ideal gas constant, T is the absolute temperature, and k_{ads} is the adsorption equilibrium constant.

Figure 7 shows the adjustment corresponding to the best adsorption model, which was the Langmuir. This model provided a good linear adjustment for the β-amino acids [47].

After performing the corresponding adjustment with the adsorption model (Table 5) and according to the literature using the values for Gibbs standard energy for adsorption for compounds **1** and **3,** it was found that the adsorption process is mixed (physisorption-chemisorption) [48-50]. However, for compound **2,** the interaction of the inhibitor with the metallic surface is chemisorption [51-54].

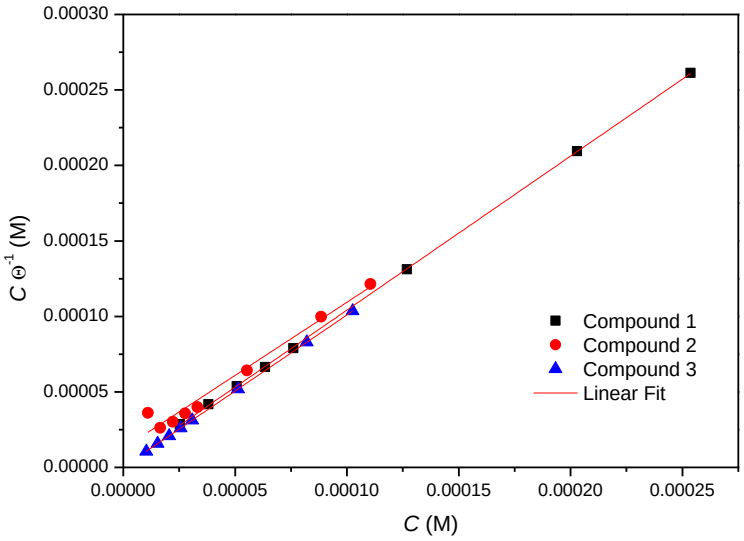

Figure 7. Langmuir adsorption isotherm for the β-amino acids on API 5L X52 steel immersed in 1 M HCl

Table 5. Thermodynamic parameters of the β-amino acids on API 5L X52 steel immersed in 1 M HCl

Compound	Ln k_{ads}	$\Delta G°_{ads}$ / KJ mol^{-1}	R^2 (correlation coefficient)
1	17.13	-38.92	1
2	19.44	-44.15	1
3	15.52	-35.26	0.99

3.5. SEM-EDS

Figure 8 shows images from SEM of the API 5L X52 steel surface, including polished images later immersed in 1 M HCl and in presence of the best inhibitor (compound **3**) at 50 ppm, as well as the corrosive environment for a 24-hour immersion.

Comparing both figures 8A and 8B, the latter shows strong damage on its surface as the result of no inhibitor presence. Nevertheless, in figure 8C, compound **3** is shown to have surface protective properties, revealing that the protective film is responsible for decreasing the damage. Finally, the

chemical analysis demonstrated that the corrosive species (oxygen and chloride ions) quantitatively decreased in the presence of compound **3**.

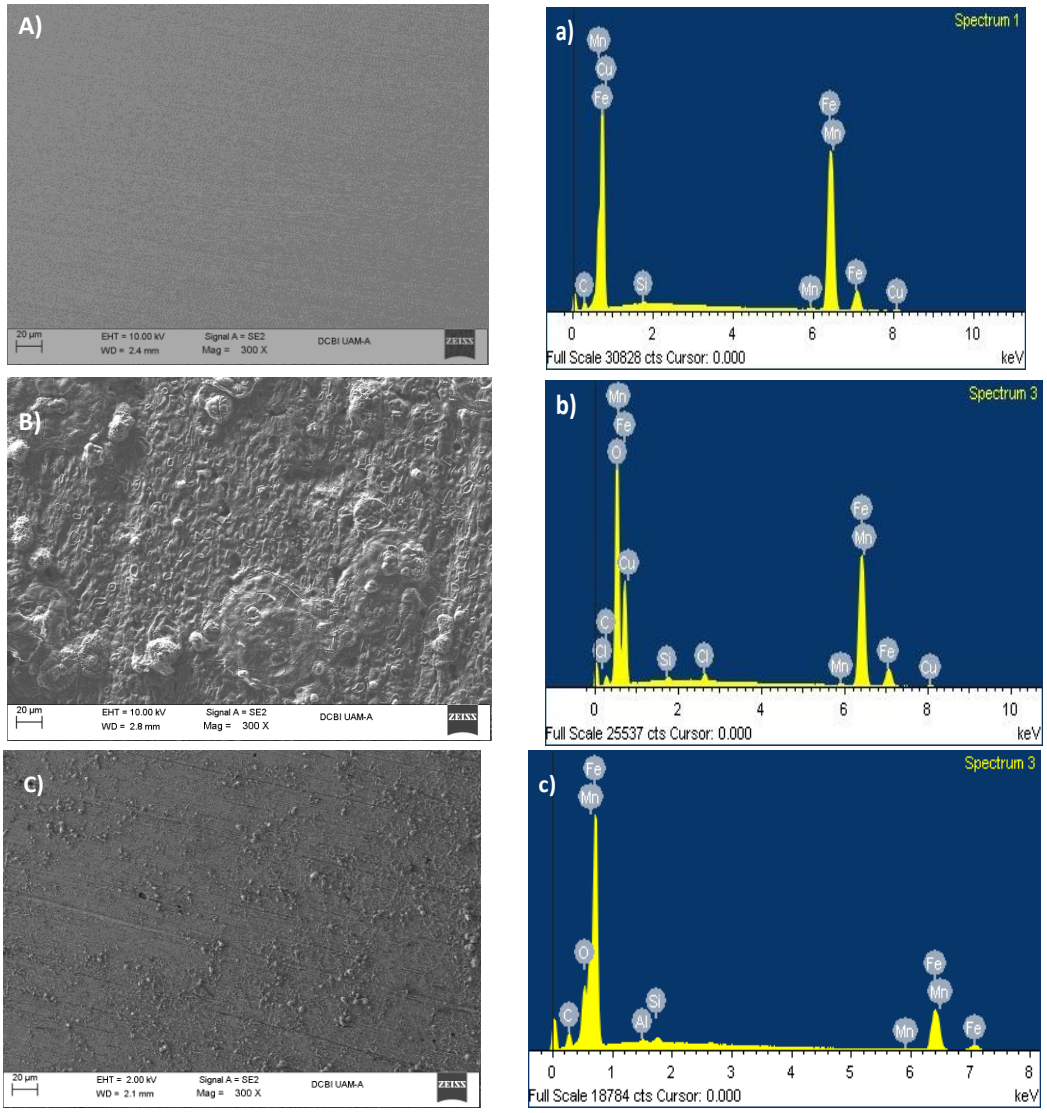

Figure 8. SEM micro-photographs of API 5L X52 steel for samples and chemical analyses: A) and a) polished and immersed in 1 M HCl, B) and b) without inhibitor, and C) and c) in the presence of compound 3.

4. CONCLUSIONS

The results clearly reveal that β-amino acids are efficient corrosion inhibitors for steel in an acid medium. Compound **1** is the best corrosion inhibitor; structurally, it has the highest number of nitrogen atoms, which promote the adsorption of the inhibitor. β-amino acids follow the Langmuir isotherm, with compound **2** operating via chemisorption and compounds **1** and **3** exhibiting a mixed process. The results of the polarization curves and electrochemical impedance spectroscopy show similar results.

The persistence of the best inhibitor (compound **1**) for long immersion times showed good protection, up to 224 hours, with $\eta \tilde{}$ 90%.

ACKNOWLEDGEMENTS
AEV and FJRG express their gratitude to the Facultad de Química (UNAM), Departmento de Ingeniería Metalúrgica and CONACyT for providing a postdoctoral fellowship.
The authors would like to thank Consejo Nacional de Ciencia y Tecnología, CONACyT (project 181448) for their financial support. We also wish to acknowledge the SNI (Sistema Nacional de Investigadores) for the distinction of their membership and the stipend received.
We thank the Divisional Electronic Mycroscopy Lab (Laboratorio Divisional de Microscopía Electrónica) for the use of SUPRA 55 VP.

References

1. P. B. Raja, M. G. Sethuraman, *Mater. Lett*., 62 (2008) 113.
2. F. S. De Souza, A. Spinelli, *Corros. Sci*., 51 (2009) 642.
3. H. Liu, T. Gu, G. Zhang, W. Wang, S. Dong, Y. Cheng, H. Liu, *Corros. Sci*., 105 (2016)149.
4. Z. Hu, Y. Meng, X. Ma, H. Zhu, J. Li, C. Li, D. Cao, *Corros. Sci.*, 112 (2016) 563.
5. Y. Qiang, S. Zhang, L. Guo, X. Zheng, B. Xiang, S. Chen, *Corros. Sci*., 119 (2017) 68.
6. H. Hamani, T. Douadi, M. Al-Noaimi, S. Issaadi, D. Daoud, S. Chafaa, *Corros. Sci.*, 88 (2014) 234.
7. N. Soltani, M. Behpour, E. E. Oguzie, M. Mahluji and M. A. Ghasemzadehb, *RSC. Adv*., 5 (2015) 11145.
8. A. Espinoza, G. E. Negrón, D. Angeles, H. Herrera, M. E. Palomar, M. A. Romero, *Int. J. Electrochem. Sci*., 9(2014) 493.
9. S. M. Shaban, *RSC. Adv*., 6 (2016) 39784.
10. M. Shabani, M. Behpour, F. S. Razavi, M. Hamadanian and V. Nejadshafiee, *RSC. Adv.*, 5 (2015) 23357.
11. a) R. González, A. Espinoza, G. E. Negrón, M. E. Palomar, M. A. Romero, R. Santillán Molecules., 18 (2013) 15064. b) A. Espinoza, G.E. Negrón, R. González, D. Angeles, H. Herrera, M. Romero, M. Palomar, *Mater. Chem. Phys*., 145 (2014) 407.
12. a) Q. Deng, N.N. Ding, X.L. Wei, L. Cai, X.P. He, Y.T. Long, G.R. Chen, K. Chen, *Corros. Sci*., 64 (2012) 64 b) Q. Deng, H. Wei Shi, N. Ding, B. Chen, X. He, G. Liu, Y. Tang, Y. Long, G. Chen, *Corros. Sci.*, 57 (2012) 220, c) Q. Deng, X.P. He, H.W. Shi, B.Q Chen, G. Liu, Y. Tang, Y.T. Long, G.R. Chen, K. Chen, *Ind. Eng. Chem. Res*., 51 (2012) 7160.
13. M. Escudero, A. Vega, E. Juaristi, *Curr. Top. Med. Chem*., 14 (2014)1257.
14. M. T. Saraiva, B. S. Martins, R. Beal, P. F. B. Gonçalves, F. S. Rodembusch, D. Alves and D. S. Lüdtke, *J. Org. Chem*., 83 (2018) 1348.
15. M. Allaoui, A. Cheriti, N. Gherraf, E. Chebouat, B. Dadamoussa, R. Salhi, *Int. J. Electrochem. Sci*., 8 (2013) 9429.
16. K.R. Ansari, M.A. Quraishi, A. Singh, *Corros. Sci.*, 79 (2014) 5.
17. A. Singh, Y. Lin, W. Liu, D. Kuanhai, J. Pan, B. Huang, C. Ren, D. Zeng, *J. Taiwan Inst. Chem. Eng.*, 45 (2014) 1918.
18. S. Javadiana, A. Yousefia, J. Neshatib, *Appl. Surf. Sci*., 285P (2013) 674.
19. S. A. Umoren, I. B. Obot, A. Madhankumar, Zuhair M. Gasem, *Carbohydr. Polym.*, 124 (2015) 280.
20. L. Feng, H. Yang, F. Wang, *Electrochim. Acta*, 58 (2011) 427.

21. K.R. Ansari, M.A. Quraishi, *J. Taiwan Inst. Chem. Eng.*, 54 (2015) 145.
22. C. Bhan, M.A.Quraishi, A. Singh, *J. Taiwan Inst. Chem. Eng.*, 49 (2015) 229.
23. H. Hamani, T. Douadi, M. Al-Noaimi, S. Issaadi, D. Daoud, S. Chafaa, *Corros. Sci*., 88 (2014) 234.
24. K. Zhang, B. Xu, W. Yang, X. Yin, Y. Liu, Y. Chen, *Corros. Sci*., 90 (2015) 284.
25. K. M. Ismail, *Electrochim. Acta*, 52 (2007) 7811.
26. A. Popova, M. Christov, A. Vasilev, *Corros. Sci*., 94 (2015) 70.
27. M. Hussein, M. F. El-Hady, H. A. H. Shehata, M. A. Hegazy, H. Hefni, *J. Surfactants Deterg.*, 16 (2013) 233.
28. C. Rahal, M Masmoudi, R. Abdelhedi, R. Sabot, M. Jeannin, M. Bouaziz, P. Refait, *J. Electroanal. Chem.*, 769 (2016) 53.
29. E. S. Meresht, T. S. Farahani, J. Neshati, *Corros. Sci*., 54 (2012) 36.
30. K. Hu, J. Zhuang, C. Zheng, Z. Ma, L. Yan, H. Gu, X. Zeng, J. Ding, *J. Mol. Liq*., 222 (2016)109.
31. S. Fouda, M.A. Ismail, G.Y. Elewady, A.S. Abousalem, *J. Mol. Liq*., 240 (2017) 372.
32. C. Verma, M.A. Quraishi, E.E. Ebenso, I.B. Obot, A. El Assyry, *J. Mol. Liq*., 219 (2016) 647.
33. K. R. Ansari, M. A. Quraishi, A. Singh, S. Ramkumard and Ime B. Obot, *RSC. Adv.*, 6 (2016) 24130
34. A. A. Al-Amiery, M. H. Othman, T. A. Abdullah, T. S. Gaazd, A. H. Kadhumb, *Results Phys.*, 9 (2018) 978.
35. A. A. Farag, M.R. Noor, *Corros. Sci.*, 64 (2012) 174.
36. M. El Azzouzi, A. Aouniti, S. Tighadouin, H. Elmsellem, S. Radi, B. Hammouti, A. El Assyry, F. Bentiss, A. Zarrouk, *J. Mol. Liq*., 221 (2016) 633.
37. G. Ji, S. Anjum, S. Sundaram, R. Prakash, *Corros. Sci.*, 90 (2015) 107
38. K. Boumhara, M. Tabyaoui, C. Jama, F. Bentiss, *J. Ind. Eng. Chem.*, 29 (2015) 146
39. M. Chellouli, D. Chebabea, A. Dermaja, H. Erramlia, N. Bettacha, N. Hajjajia, M.P. Casalettob, C. Cirrincioneb, A. Priviterab, A. Srhiric, *Electrochim. Acta.*, 204 (2016) 50
40. A. Odewunmi, S.A. Umoren, Z.M. Gasem, *J. Environ. Chem. Eng.*, 3 (2015) 286.
41. Y. Qiang, S. Zhang, B. Tan, S. Chen, *Corros. Sci.*, 133 (2018) 6-16
42. R. Karthikaiselvi, S. Subhashini, *Arabian J. Chem*., 10 (2017) S627.
43. A. J. Abdul, M. A. Sathiq, *Arabian J. Chem*., 10 (2017) S261.
44. K. Zakaria, A. Hamdy, M.A. Abbas, O.M. Abo, *J. Taiwan Inst. Chem. Eng.*, 6 (2016) 530.
45. L. O. Olasunkanmi, M. M. Kabanda, E. E. Ebenso, *Phys.*, E76 (2016) 109.
46. M. A.J. Mazumder, H. A. Al-Muallem, M. Faiz, S. A. Ali, *Corros. Sci*., 87 (2014) 187.
47. K. Wan, P. Feng, B. Hou and Y. Li, *Rsc. Adv.*, 6 (2016) 77515.
48. P. B. Raja, A. K. Qureshi, A. A. Rahim, H. Osman, K. Awang, *Corros. Sci*., 69 (2013) 292.
49. B. Mernari, H. El Attari, M. Traisnel, F. Bentiss, M. Lagrenee, *Corros. Sci*., 40 (1998) 391.
50. A. Ali Sk, M. T. Saeed, S. U. Rahman, *Corros. Sci.*, 45 (2003) 253.
51. S. A. Ali, H. A. Al-Muallem, S. U. Rahman, M. T. Saeed, *Corros. Sci*., 50 (2008) 3070.
52. D. K. Singh, S. Kumar, G. Udayabhanu, P. J. Rohith, *J. Mol. Liq*., 216 (2016) 738.
53. M. ElBelghiti, Y. Karzazi, A. Dafali, B. Hammouti, F. Bentiss, I. B. Obot, I. Bahadur, E. E. Ebenso, *J. Mol. Liq.*, 218 (2016) 281.
54. G. Karthik, M. Sundaravadivelu, P. Rajkumar, *Res. Chem. Intermed*., 41(2015) 1543.